PHYSICAL REVIEW B VOLUME 24, NUMBER 10 15 NOVEMBER 1981

Elastic core effect in Al-Mg alloys by extended x-ray absorption fine structure in the soft-x-ray range

D. Raoux, A. Fontaine, P. Lagarde, and A. Sadoc
*Laboratoire pour l'Utilisation du Rayonnement Electromagnétique,**
Université Paris Sud, Bâtiment 209 C, 91405 Orsay, France
and Laboratoire de Physique des Solides,†
Université Paris Sud, Bâtiment 510, 91405 Orsay, France
(Received 14 January 1981)

The extended x-ray absorption fine structure (EXAFS) spectra of Al−3 at. % Mg and Al−7 at. % Mg have been measured on the magnesium K edge (1303 eV) using the soft-x-ray beam delivered by the ACO (Anneau de Collision d'Orsay) storage ring, as well as the EXAFS of elemental aluminium (1556 eV) and magnesium. With the use of quasiexperimental phase shifts determined from aluminum and magnesium data, the first-shell radius around a magnesium impurity in an Al-Mg alloy has been determined within ± 0.015 Å, yielding a direct measurement of the elastic core effect which turns out to be large ~ 0.08 Å. It is discussed in the framework of the elastic theory of continuous media and of the lattice static method, both of which fail to give the correct magnitude of the local relaxation.

I. INTRODUCTION

Point defects such as solute atoms dispersed at random in a substitutional solid solution expand or contract the host lattice and change the average lattice parameter a. At least for low concentrations c, the dependence on c is linear (Vegard's law) and the slope da/ac measures the macroscopic effect due to the strains induced in the matrix by the solution atoms. However, the local effect which drives it, the so-called elastic core effect around the impurity, could not be measured until recently when it became possible using the EXAFS technique (extended x-ray absorption fine structure). As it has been pointed out by various authors[1−3] even in the conventional transmission mode, EXAFS may give the local environment of a specific atom in a dilute system by exciting its own K or L absorption spectrum which does not overlap the EXAFS spectra of the other components. It thus has been used to measure directly the displacement of the atoms of the first shell around an impurity in dilute Al-Cu (Ref. 4) and Al-Zn (Ref. 5) alloys. These first measurements of the core effect have raised a question concerning its connection to the macroscopic effect measured by the change of the lattice parameter, since they are about 3 times larger than the value one can calculate from the slope of the Vegard's law using the elastic theory of continuous medium and the experimental values of da/ac. In the case of Al-Cu alloys, the EXAFS measurement of the core effect is -0.125 ± 0.01 Å, which is much larger than the experimental uncertainty. For Al-Zn alloys it is only -0.02 ± 0.01 Å so that the discrepancy between the EXAFS measurement and the value calculated from the relative change of parameter is less significant. This failure of the elastic theory of continuous medium when used in the vicinity of a defect can in principle be bypassed by the lattice static method,[6,7] which takes into account the discrete character of the lattice. It, however, requires the knowledge of the impurity-host potential, which makes it difficult. To our knowledge, it has not been used to calculate the strains in Al-Cu and Al-Zn solid solutions, but there is a calculation for Al-Mg by Tomlinson *et al.*[8] It suggests a very weak displacement $db\sim 0.02$ Å of the aluminium atoms surrounding the magnesium impurity, while from the slope of the Vegard's law we can calculate a value of about 0.04 Å, which is twice as large, as will be discussed in Sec. V. It is thus very interesting to perform the EXAFS measurement of the core effect in Al-Mg solid solutions in order to compare both theoretical values with the experimental determination.

There are also other reasons to choose Al-Mg alloys for such a measurement. First, it is possible

to make solid solutions up to rather large magnesium concentrations ($\sim 10\%$); then the magnesium atoms expand the aluminium host matrix, while zinc and copper atoms contract it. However, EXAFS measurements on the magnesium K edge (1303 eV) are much more difficult than on the copper or zinc K edges, which are at about 10 keV. We deal here with the soft-x-ray spectroscopy, which has been less developed for various technical reasons[9]: lack of efficient monochromators and detectors, and very high absorption of x rays by matter which makes the use of very thin samples necessary. Moreover, the analysis of the EXAFS spectra of the magnesium impurity in a dilute Al-Mg sample is more delicate than that of copper or zinc in the same Al matrix because the K-edge absorption of aluminium occurs at 1559.3 eV, at about 250 eV above the edge of magnesium. We then have to analyze data in a rather narrow energy range for which the EXAFS theory is not as well established as it is for higher energies. For this reason, great care has to be taken in the data handling in order to get a correct determination of the first shell radius. These points will be discussed in Secs. III and IV of this paper, which deal, respectively, with the method of analysis of the spectra and the accuracy of the results. A discussion of the results is given in Sec. V, while Sec. II is devoted to the experimental techniques.

II. EXPERIMENTAL TECHNIQUES

A. Elaboration of the samples

Samples have been prepared from large ingots (50 g) of Al—3 at. % Mg and Al—7 at. % Mg kindly supplied by the Laboratoire de Métallurgie Physique (Poitiers). Chemical composition has been measured by Castaing's microprobe analysis and turns out to be 3.0 and 7.3 at. %. Strips of about 10 μm have been made by five successive steps of rolling, each of them being performed after an annealing at 350 °C during 2 h in a secondary vacuum. After the final rolling, the samples have been once more annealed at 350 °C for 2 h and quenched in an argon-gas flow, so that any clustering produced by the rolling stages is eliminated since Guinier-Preston (GP) zones in Al-Mg alloys disappear in a few minutes by annealing.[10] Finally, the correct thicknesses have been obtained by thinning the samples down to a few micrometers in a NaOH solution for 1.5 h at room temperature. From the magnitude of the jump at the K edge of magnesium, and by comparison with the absorption of a 2-μm thick magnesium foil, we can estimate the actual thicknesses of our samples to about 5 μm. Our samples have been kept at room temperature before the EXAFS measurements for periods ranging between two and four weeks. This should not give any clustering of the magnesium atoms as has been shown by various studies. Since this is a crucial point, we recall briefly that resistivity measurements by Dauger[10] show that there is no clustering of magnesium atoms at room temperature for Al—9 at. % Mg samples, while there is a GP zone formation for Al—13 at. % Mg alloys. Moreover, by using small-angle neutron scattering, Roth and Raynal[34] did not find any GP zones in Al—7 at. % Mg alloys aged one year at room temperature or even at 40 °C, while they detected a ring characteristic of the GP zones for Al—11.5 at. % Mg alloys. Both studies do suggest strongly that magnesium atoms do not cluster if their concentration is lower than 9 at. % when the sample is kept at room temperature. This conclusion is also supported by an x-ray scattering study by Dauger, Guillot, and Caisso[24] performed on more concentrated samples (11.5 and 13 at. % Mg). GP zones then give rise to x-ray diffuse extrareflections on both sides of Bragg peaks. From the analysis of their profiles, they got a modeling of the zones which implies that about 8 at. % of the magnesium atoms are still dispersed in the matrix. All these studies show convincingly that there is no magnesium clustering in samples kept at room temperature for concentrations lower than 7 at. %. This assumption is still reinforced for the Al—3 at. % Mg sample.

B. EXAFS experiments

The EXAFS experiments were performed at the French synchrotron radiation center LURE (Laboratoire pour l'Utilisation du Rayonnement Electromagnetique) using the soft-x-ray beam delivered by the ACO (Anneau de Collision d'Orsay) storage ring. ACO was operated at 540 MeV, with a beam current between 50 and 200 mA. The experimental setup has been described elsewhere.[11,9] The Bragg monochromator is a two-crystal device with parallel mounting, the position of the outgoing beam being kept constant by monitoring the distance between the crystals. The crystals used were potassium acid phthalate (KAP) plates with a $2d$ spacing of 26.63 Å. Absorption measurements on

the K edge of aluminium have been performed using an ion chamber filled with 300 Torr of air; on the magnesium K edge, we have used a channel plate as a detector, since for that energy range, the signal-to-noise ratio is better. A thin 10-μm beryllium foil was used as a filter cutting off the visible and uv intense light emitted by ACO. The entire experiment is monitored by a Tektronix 4051 computer.

In the energy range between 1200 and 2000 eV, the resolution of the monochromator is poor, typically 4 eV, because of the small Bragg angle due to the large $2d$ spacing of the KAP crystal. It is, however, sufficient for an EXAFS analysis. Thus photon energies have only been swept by 2-eV steps. The photon energies have been calibrated with the inflection points of the Al and Mg K edges at, respectively, 1559.3 and 1303 eV. The intensities I transmitted through the sample and I_0 without the sample were recorded through successive 30-min runs, since it is not possible to monitor I_0 with an ion chamber because of the very large absorption of soft x rays by matter. I and I_0 were then corrected for the drop in intensity of the ACO electron beam, which was typically 15% per hour. Experiments have been made at liquid-nitrogen temperature, in order to reduce the Debye-Waller damping of the EXAFS spectra using a cold-finger cryostat. Typical experimental absorption curves are shown in Fig. 1 (raw data). They have been obtained in about 30 min at 80 K. The signal-to-noise ratio is rather poor, especially for the dilute Al-Mg samples for which there is a large background absorption due to the aluminum matrix. In order to improve the quality of the data, several experiments have been averaged (up to 15 for the Al-Mg samples), yielding then the EXAFS spectra shown in Fig. 2.

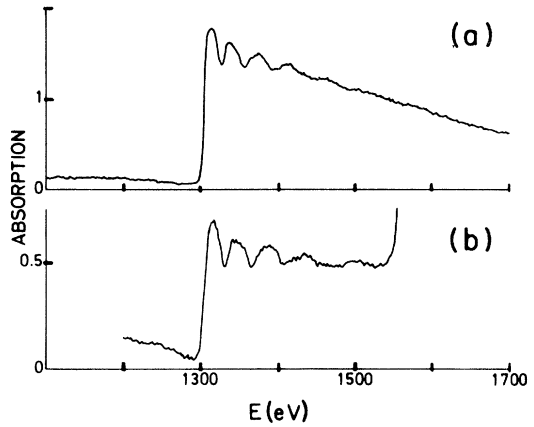

FIG. 1. Absorption spectra of (a) a 3-μm thick magnesium foil and (b) of a 20-μm thick packing of two Al—3 at. % Mg samples (raw data measured in 30 min at 78 K).

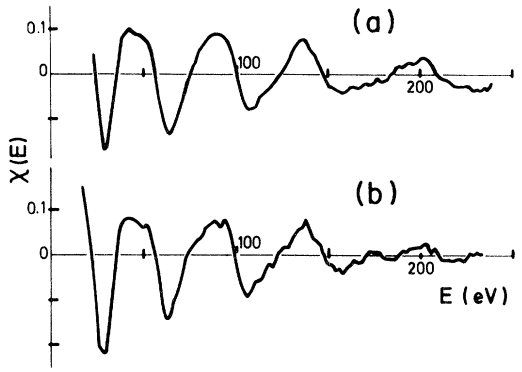

FIG. 2. EXAFS spectra of (a) Al—7.3 at. % Mg and (b) Al—3.0 at. % Mg samples on the magnesium K edge ($E_0=1303$ eV).

III. METHOD OF ANALYSIS OF THE SPECTRA

A. Quasiexperimental determination of the phase shifts

The aim of this paper is restricted to the measurement of the distance between a magnesium atom and its nearest neighbors. We thus only deal with the phase of the EXAFS signal and will not discuss its amplitude. In the one-electron theory, if multiple-scattering effects are neglected, the phase of the modulations due to a shell of j atoms at a distance R_j from the central atom is given by the now-classical theory[12—14]

$$\varphi_j(R_j,k)=2kR_j+2\delta_1'(k)+\arg f_j(\pi,k)\ , \qquad (1)$$

where k is the photoelectron momentum which is given in atomic units by

$$k=[(E-E_0)/13.605]^{1/2}\ . \qquad (2)$$

E and E_0 in eV are, respectively, the energy of the impinging photon and the origin of kinetic energy of the photoelectron, $2\delta_1'(k)$ is the phase shift in the central magnesium atom due to the hole in the K shell, and $\arg f_j(\pi,k)$ is the phase of the backscattering of the electron by the jth atoms.

Even for a perfect substitutional solid solution, at 3 and 7 at. % concentrations the first shell is not

homogeneous and includes, respectively, 0.36 and 0.84 magnesium atom which may be at a distance larger than the aluminium atoms. The EXAFS measurement will only give us the mean radius of the first shell without discriminating Mg and Al neighbors. Moreover, the backscattering phase shift depends on the atomic number of the backscattering: For Mg it is lower by about 0.4 rad than that for Al,[15] and the slope of the phase is smaller by about 2×10^{-2} rad/Å^{-1} in the energy range of interest. Then using the backscattering phase shift of aluminium for an Al—7 at. % Mg alloy, we overestimate the actual slope by about 1.4×10^{-3} rad/Å^{-1} and thus get an average distance which is smaller by about 7×10^{-4} Å than the actual value. This is well beyond the accuracy of the EXAFS analysis and can be completely neglected.

We can only analyze data over about 230-eV range between the K edges of magnesium and aluminium. In such a low energy range, the EXAFS simple theory which results in Eq. (1) is not as good as it is at higher energies. Lee and Pendry[16] have shown that the plane-wave approximation has then to be relaxed. Moreover, chemical effects which are not taken into account in the calculation of the phase shifts become important, as well as the screening of the hole by intra-atomic processes[17] or by conduction electrons.[18] In the case of aluminium[9] we have shown previously that this last effect could result in an underestimation of the nearest-neighbor distance by 0.06 Å at $E<130$ eV when using the phase shifts calculated by Lee and Beni[19] for an unscreened central atom.

The use of theoretical values for the atomic phase shifts may thus be dangerous in this case, and it is safer to meaure the phase shifts from the EXAFS of model compounds and use them in the analysis of the Al-Mg spectrum. The chemical transferability of the phase shifts is now well established, at least when the chemical state and the local environment are similar.[20] However, we do not have a model compound which simulates the aluminium environment of the magnesium solute atoms. We had to use pure metallic aluminium and magnesium data and determine the corresponding φ_{Mg} and φ_{Al} phase shifts. Then we have simulated the $\varphi_{\mathrm{Mg\text{-}Al}}$ phase shift associated to a Mg-Al pair, where Mg is the central atom and Al the backscatterer, by

$$\varphi_{\mathrm{Mg-Al}}=\varphi_{\mathrm{Mg}}+[\arg f_{\mathrm{Al}}(\pi)-\arg f_{\mathrm{Mg}}(\pi)]$$
$$=\varphi_{\mathrm{Al}}+(2\delta'_{1,\mathrm{Mg}}-2\delta'_{1,\mathrm{Al}})\ . \qquad (3)$$

Since the phase shifts vary slowly with the atomic number, the differences of the backscattering phases or of the central atom phase shifts for Al and Mg ($\Delta Z=1$) are very weak. They can then be approximated with safety using calculated phase shifts from Teo and Lee,[15] since all systematic errors are mostly cancelled out in differences. Using this procedure, we get two sets of quasiexperimental phase shifts which should be very similar. This will be discussed in Sec. IV.

B. Data handling

Data were analyzed using the usual method of Fourier filtering and details on our data handling procedure have been previously published.[4,21] We have carefully studied the influence of the windows used in both $\vec{k}$ and $\vec{R}$ space in the Fourier filtering process since the EXAFS signal for Al-Mg alloys is restricted to a low-energy range $E<230$ eV for which small changes in the locations of the zeros may result in rather large changes in the determination of the distance ($\Delta R/R\sim\Delta k/k$).

The EXAFS spectra shown in Figs. 2(a), 3(a), and 4(a) have been Fourier transformed after multiplication by the momentum k, using several smooth windows with k_{min} ranging from 2 to 4.5 Å^{-1} and k_{max} from 8 to 12 Å^{-1}. The main peak in the $\vec{R}$ space is then isolated [Figs. 3(b), 4(b), and 5(b)] and back transformed to the $\vec{k}$ space, yielding then a partial EXAFS signal [Figs. 3(a), 4(a), and 5(a)]. Here again, several windows have been used to isolate the main peak in the $\vec{R}$ space, some of them including the small bumps on the low distance sides. The partial EXAFS signals indeed do not depend much on the range of k values used, at least as far as the phases are concerned. The amplitudes do change in the low-energy part of the spectrum when k_{min} is lowered towards 2 Å^{-1}. This reflects the strong increase of the backscattering amplitude for low-Z elements when decreasing k. Using or not the bump on the low distance side of the main peak in the $\vec{R}$ space does change the phase of the partial EXAFS signal. However this change is rather weak. As an example, in the case of pure magnesium, the phases of the various filtered EXAFS we get using different windows in $\vec{k}$ or $\vec{R}$ space all lie within a 0.3-rad range. In a distance determination, this would give a spread of about 0.025 Å at 150 eV and 0.015 Å at 400 eV. This shows that, even when EXAFS can only be measured over 200 or 300 eV, a reasonable accuracy may be reached.

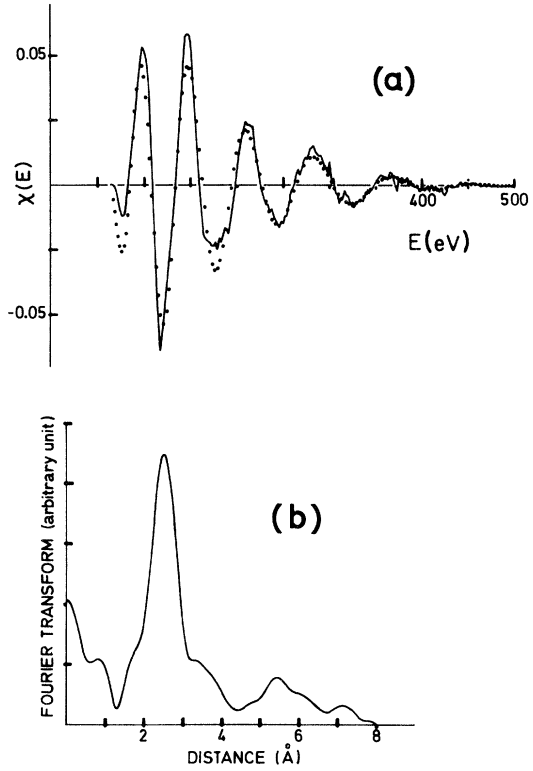

FIG. 3. (a) EXAFS spectrum of a 1-μm thick aluminium foil at 78 K (solid line) and Fourier filtering of the first-shell contribution (dots). (b) Amplitude of the Fourier transform.

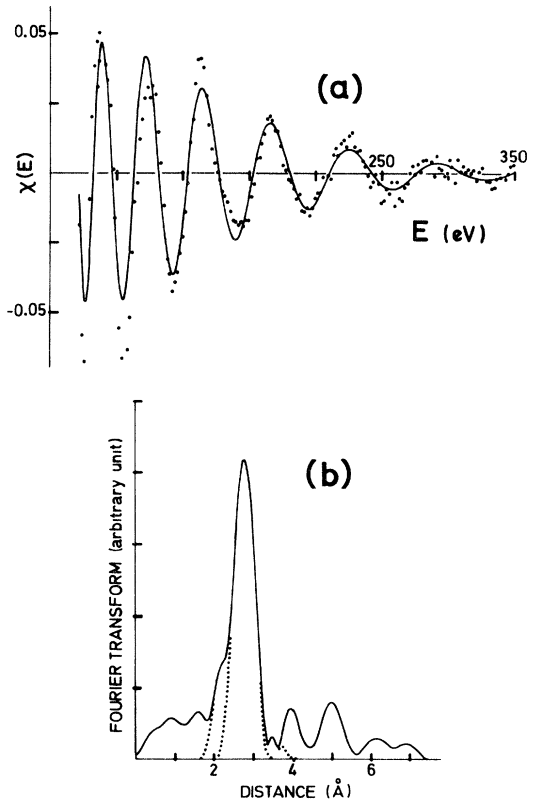

FIG. 4. (a) EXAFS spectrum of a 3-μm thick magnesium foil at 78 K (dots) and Fourier filtering of the first-shell contribution (solid line). (b) Amplitudes of the Fourier transform. Dots show various trials to isolate the first main peak.

IV. EXAFS RESULTS

The three EXAFS curves shown in Figs. 3(a), 4(a), and 5(a), which correspond, respectively, to pure aluminium, pure magnesium, and the Al−3 at.% Mg dilute alloy, have similar shapes which are characteristic of the compact structures (fcc or hcp). Fourier transforms [Figs. 3(b), 4(b), and 5(b)] exhibit the contributions of several shells. The fourth shell gives an enhanced signal which can be attributed to the so-called shadowing effect which has been discussed by Lee and Pendry.[16] This could give some information on the relaxation of the Al matrix at the fourth shell around the solute.

The main peak in Al is found at 2.505 Å, at 0.35 Å from the first-neighbor distance $d=2.854$ Å; this translation comes from the average slope of the atomic phase shift φ_{Al}. In pure Mg, this translation is 0.42 Å. In Al-Mg alloys the first peak is found at 2.54 Å. Since the $\varphi_{\mathrm{Mg\text{-}Al}}$ phase shift is intermediate between φ_{Al} and φ_{Mg}, the ΔR translation should be close to $(0.35+0.42)/2=0.385$ Å. This gives a rough but very direct determination for the first-shell radius around Mg in Al-Mg of 2.925 Å, with an uncertainty lower than ± 0.03 Å.

A. Determination of the phase shift from data on aluminium and magnesium

A comparison of the present data on aluminium which have been measured at ~ 80 K with those previously published, which were obtained at room temperature,[9] shows the drastic effect of temperature on the Debye-Waller damping at $E>200$ eV. At 80 K the spectrum extends over 500 eV, while at room temperature it is restricted to a 250-eV range above the edge. Indeed not only the amplitudes are changed, but also to a less extent the phases at E larger than 200 eV. This is probably

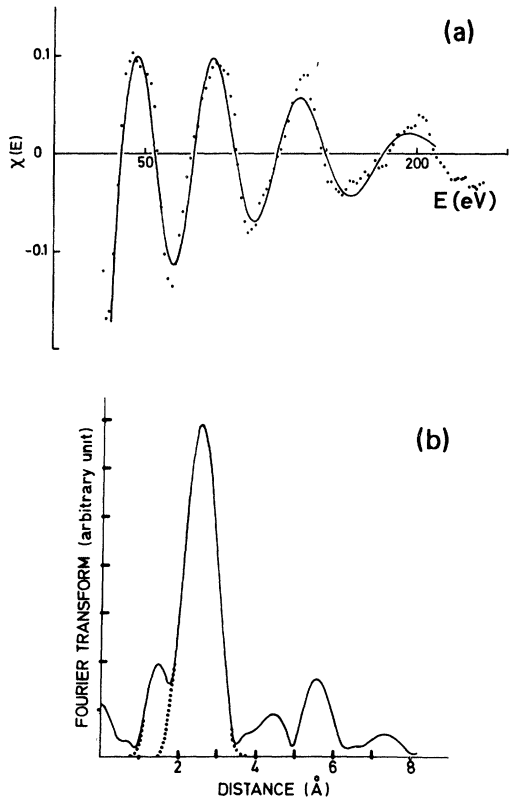

FIG. 5. (a) EXAFS spectrum (· · ·) and first-shell Fourier filtering (——) of an Al—3 at. % Mg sample (experiments performed at 78 K). (b) Amplitude of the Fourier transform. Dots show the two different ways used to isolate the first main peak.

due to an asymmetrical distribution of the distances in the first coordination shell at room temperature, resulting from the anharmonicity of vibrations. A similar, though much larger, effect has been discussed by Eisenberger and Brown[22] for zinc.

From the locations of the zeros of the filtered first-shell EXAFS, we can determine the atomic phase shifts, since the overall phase $\varphi_j(R_j,k)$ is then equal to $n\pi$. From data on elemental aluminium and magnesium we thus get two sets of values which are shown in Fig. 6 for, respectively, $\varphi_{\mathrm{Al}}(+)$ and $\varphi_{\mathrm{Mg}}(\Delta)$, the origin of k being at the inflection point of the absorption edges. The curves showing their k dependence have very similar slopes and may be deduced from each other by roughly a translation of 1 to 1.5 rad. We then try to simulate the $\varphi_{\mathrm{Mg\text{-}Al}}$ phase shift associated with a Mg-Al pair of atoms as discussed in Sec. III, and we use theoretically calculated values given by Teo and Lee[15] to estimate the change in the central-atom phase shift ($2\delta_1'$) or in the backscattering phase $\arg f(\pi)$. These corrected phase shifts, which are also shown in Fig. 6, are now very close since they only differ by 0.2 to 0.4 rad. However, the values determined from the aluminium data are systematically larger than those determined from the magnesium values: This is due to an incorrect choice of the E_0 zero of the kinetic energies. Indeed, E_0 should not be taken at the Fermi level, which is given by the inflection point on the absorption edge, but at a lower energy, since at the Fermi level an electron in a metal has already a kinetic energy. E_0 should be at the bottom of the conduction band in a free-electron-like metal. Since Al and to a lesser extent Mg are very simple metals with conduction bands close to a free-electron one, it is better to choose for E_0 the bottom of the conduction bands at 11.7 and 7.1 eV below the Fermi level in Al and Mg. This decreases the phase shifts, as shown in Fig. 6. The two determinations for $\varphi_{\mathrm{Mg\text{-}Al}}$ are then the same within experimental errors. This gives us great confidence in the validity of our determination of $\varphi_{\mathrm{Mg\text{-}Al}}$. Moreover, it shows that E_0 indeed is not an adjustable parameter, but has a physical meaning: E_0 should be taken at the bottom of a free-electron-like band which fits the conduction band at high energies. This value is of course close to the bottom of the conduction band in a free-electron-like metal Al, or even Mg.

B. Measurement of the first-shell radius in Al-Mg alloys

As shown in Fig. 2, EXAFS spectra for 3- and 7-at. % Mg concentrations are very similar, showing no evidence for GP zones formation in the more concentrated alloy. This is in good agreement with previous studies by other techniques.[10].

From the k values of the nodes of the filtered EXAFS, one can determine a set of values of the first shell radius R_k since one has

$$2kR_k+\varphi_{\mathrm{Mg\text{-}Al}}(k)=n\pi\ , \tag{4}$$

where n increases by one at each node.

We use the $\varphi_{\mathrm{Mg\text{-}Al}}$ values calculated with E_0 at the bottom of the conduction bands in Al and Mg. Of course, the R values depend on the choice of the E_0 reference energy for Al-Mg. We then follow a procedure first suggested by Martens *et al.*[23]: We vary E_0 for the Al-Mg data until we get the

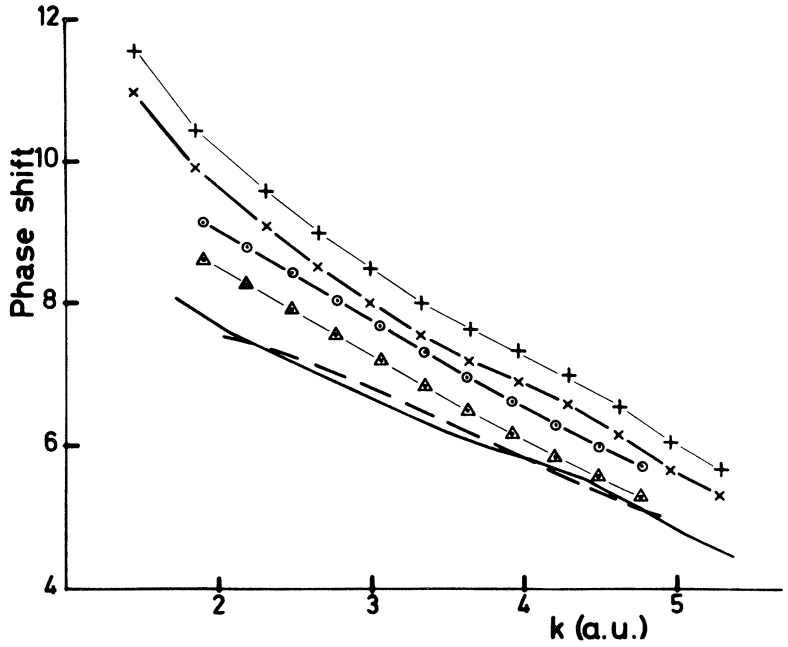

FIG. 6. Phase shift versus electron momentum. Experimental determinations of aluminium (+) and magnesium (Δ) phase shifts, the zero of kinetic energy being taken at the inflection point of the K edges. Corrected phase shifts which simulate a Mg-Al pair, Mg being the central atom. ×, results from the aluminium data corrected for the central atom, and ○, from the magnesium data corrected for the backscatterer. The origin of kinetic energy is taken at the inflection point of the edges. The two lowest curves show the same phase shifts with zero energy taken at the bottom of the conduction bands, i.e., 7.1 eV below the magnesium edge (— — —) and 11.7 eV below the aluminium edge (——).

flattest curve for the k dependence of the values. This gives the best determination R_{opt} and E_0. We also can estimate the uncertainty in our measurement in the following way[5]: For each E_0 value we calculate the standard deviation σ of the R determinations; the best choice of E_0 will give the smallest value of σ. The error bars are determined for $\sigma=\sqrt{2}\sigma_{\text{min}}$. A typical example is shown in

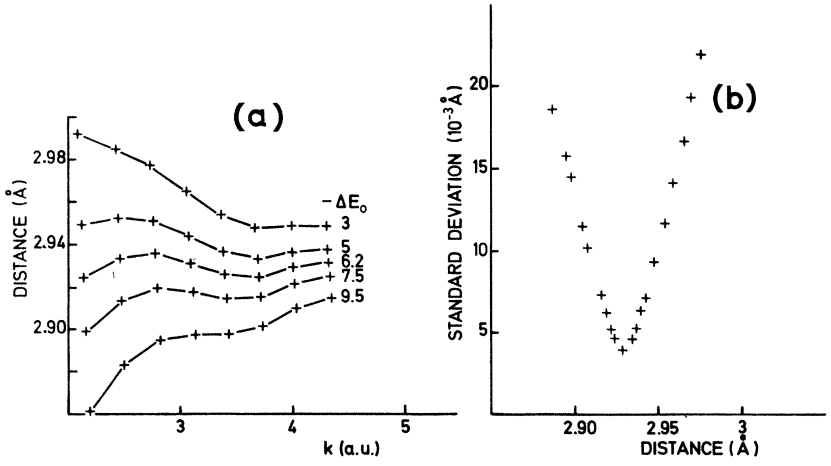

FIG. 7. (a) An example of the R vs k determination for the Al—3 at.% Mg sample for five different values of E_0, the zero of kinetic energy, ranging from 3 to 9.5 eV below the inflection point. Best choice is 6.2 eV giving $\bar{R}=2.93$ Å. (b) Standard deviation of the set of values of $R(k)$ versus the average $\bar{R}$ value for different values of E_0.

Fig. 7 for Al−3 at. % Mg data, which gives $R_{opt}=2.93$ Å, $\Delta R=\pm 0.01$ Å and $E_0=-6.2$ eV with respect to the inflection point. As is illustrated by Fig. 7(b) this procedure is rather accurate, and gives R within a ± 0.01 Å range. It has been performed for the various Fourier-filtered first-shell EXAFS for both Al−3 at. % Mg and 7 at. % Mg alloys. For each of these trials we have used values of the phase shifts $\varphi_{Al\text{-}Mg}$, which have been determined from data on both elemental aluminium and magnesium. Each Fourier-filtered Mg-Al signal was analyzed using phase shifts derived through a similar filtering process (same k and R windows). All the R_{opt} values thus determined lie in the range 2.93 ± 0.015 Å for Al−3 at. % Mg and 2.94 ± 0.015 Å for Al−7 at. % Mg alloy. We thus are pretty confident in our measurement and would like to point out here that EXAFS may give an accuracy of ± 0.02 Å even when the signal is restricted to less than 250 eV provided that experimental or quasiexperimental phase shifts are used.

The two measurements give the same value within the experimental uncertainty. This also suggests that there is no clustering of magnesium. However, as discussed in Sec. III, even in a solid solution the first shell does include some magnesium atoms, and the magnesium-magnesium pairs may contribute to the average first-neighbor distance measured by EXAFS. Our data do not give the magnesium-magnesium distance. We can get a rough estimation from the distances within the Guinier-Preston zones which are small particles formed at the first stage of annealing and containing about 25% of magnesium. X-ray scattering studies have shown that they have a fcc structure with a parameter larger than that of the aluminium matrix by 0.7%,[24] while a transmission electron microscopy measurement has given a larger value of about 5%.[25] For various reasons, this high value seems to be unlikely. Anyway the corresponding Mg−Mg distances within the zone would be 2.88 and 3.00 Å, within ± 0.06 Å from our average EXAFS measurement. For an Al−3 at. % Mg alloy, the magnesium-magnesium pairs would thus shift the average distance in the first shell by at most ± 0.002 Å and for an Al−7 at. % Mg alloy by at most ± 0.0045 Å. This effect can then be neglected since our experimental uncertainty is ± 0.015 Å. We thus believe that the average nearest-neighbor distance that we have measured by EXAFS is indeed very close to the actual nearest-neighbor distance around an isolated magnesium atom in the solid solution.

V. DISCUSSION

We have obtained here the third measurement of the elastic core effect in Al solid solutions. Thus it is now possible to discuss the three determinations of the core effect around Cu, Zn, and Mg solute atoms and compare them to the corresponding macroscopic changes in the x-ray lattice parameter using the continuous elastic theory. It has been progressively settled by various authors[26–28] who have introduced several refinements. We think it may be useful to recall here the main points of such a theory before comparing our direct measurements to the value one can deduce from the Vegard's law.

A. Continuous elastic theory for Vegard's law

Two main models have been developed to explain Vegard's law in substitutional solid solutions. In the simplest model,[27] the solute atom is taken as a sphere, the radius of which is different from that of the matrix atoms; it is forced into a spherical hole of a slightly different size. Blandin and Deplante[28] have developed a more physical model for metallic solid solutions, which takes into account the screening of the atom by conduction electrons when solute and matrix atoms have different valencies. This oscillating charge density yields an electric field which acts on the neighboring host ions; the radius of the first shell is determined by the balance between the elastic stress and the electrical force.

However, whatever the origin of the displacement db^{∞} of the first-shell atoms, the strains relax in an infinite medium following

$$u_{\infty}(r)=db^{\infty}\frac{b^2}{r^2},$$

where b is the first-shell radius.

The next step is to introduce a finite concentration of solute atoms, i.e., to give each solute atom a finite volume taken as a sphere of radius R. These contiguous volumes must be stress-free at their borders, so that image surface stresses are required to balance the stresses that would be created by one solute atom embedded in an infinite medium. These image stresses are distributed uniformly at the border surfaces, and for a large enough volume of alloy, they result in a uniform displacement

$$u_I(r)=db^{\infty}(\gamma-1)\frac{b^2}{R^2}\frac{r}{R},$$

where γ is an elastic coefficient

$$\gamma=1+\frac{4\mu\chi}{3}=3\frac{1-\sigma}{1+\sigma}$$

close to 1.5 for all metals (χ is the coefficient of compressibility, μ the shear modulus, and σ, the Poisson ratio, is 0.34 for Al). One then gets

$$u(r)=u_{\infty}(r)+u_I(r)$$
$$=\frac{db^{\infty}}{b}\frac{c}{y}\left[(\gamma-1)r+\frac{R^3}{r^2}\right]=Ar+B\frac{R^3}{r^2}\ , \tag{5}$$

where c is the atomic concentration and $y=(3/4\pi)\times(\Omega/b^3)$, Ω being the volume left to one atom in the matrix [$c/y=b^3/R^3$ since $c=(3/4\pi)(\Omega/R^3)$]. It may be noted that y only depends on the structure of the matrix (for an fcc structure $y=0.169$).

In this formulation, the compressibility of the solute atom has been taken as that of the matrix. This assumption can be relaxed, and one can treat the solute atom as a continuous medium of compressibility χ' different from that of the matrix.[29]

The constants A and B in (5) are then changed to

$$A'=A(1+\epsilon)=A\left[1+\frac{y}{\gamma'}\frac{\chi'-\chi}{\chi}\frac{1+\frac{c}{y}(\gamma-1)}{1-c\frac{\gamma-1}{\gamma'}\frac{\chi'-\chi}{\chi}}\right],$$

$$B'=B(1+\eta)=B\frac{1+\frac{y}{\gamma'}\frac{\chi'-\chi}{\chi}}{1+c\frac{\gamma-1}{\gamma'}\frac{\chi'-\chi}{\chi}}$$

with $\gamma'=1+\frac{4}{3}\mu\chi'$. For low concentrations $\epsilon\sim\eta$, and then

$$u(r)=\frac{db'^{\infty}}{b}\frac{c}{y}\left[(\gamma-1)r+\frac{R^3}{r^2}\right] \tag{6}$$

with $db'^{\infty}=db^{\infty}(1+\eta)$.

Using numerical values of the elastic constants given by Gschneider[30] for pure metals we get $\eta=0.096$ and 0.11 for, respectively, Al—3 at. % Mg and Al—7 at. % Mg alloys (and 0.13 for Al—2 at. % Cu and 0.02 for Al—0.83 at. % Zn). This correction is a rather small one. Indeed, it is probably overestimated because of the screening of the solute atom, which makes it resemble the host atom.

It is also important to point out that for a finite concentration the actual $db=u(b)$ value of the displacement of the first-shell atoms around the solute differs from db^{∞}. From (6), we get

$$db=u(b)=db'^{\infty}\left[1+\frac{\gamma-1}{y}c\right]$$

with $(\gamma-1)/y=2.96$ for Al alloys.

We then have to relate $db=u(b)$ to the relative parameter change or to the relative volume change. For a given concentration of point defects where $V=\frac{4}{3}\pi R^3$ is the average volume left to each solute atom, we have

$$\frac{\Delta V}{V}=\frac{3u(R)}{R}=\frac{3da}{a}\ ,$$

and thus

$$\frac{da}{ac}=\frac{u(R)}{cR}=\frac{\gamma}{y}\frac{db'^{\infty}}{b}=\frac{\gamma}{y}db\Big/b\left[\frac{1+(\gamma-1)c}{y}\right]. \tag{7}$$

This is the correct relationship which relates the slope of the Vegard's law to the actual displacement of the first-shell atoms surrounding a point defect.

B. Failure of the elastic theory of continuous medium in the neighborhood of a defect

Using the relationship (7) we can compare our EXAFS direct determination to the value inferred from the elastic theory of continuous medium. We use da/ac values given by Pearson,[31] which indeed do not depend on the Mg concentration up to 10%. The corresponding values of db do increase slightly with concentration, as is shown in Table I, so also the EXAFS determinations. For both 3- and 7-at. % magnesium concentrations the EXAFS measurements are about 2 times larger than the value inferred from the change in the lattice parameter. This discrepancy is larger than the uncertainty of the EXAFS measurement. For completeness we have also compared in Table I da/ac to the EXAFS measurement of the core effect we have previously performed for Al-Cu (Ref. 4) and Al-Zn (Ref. 5) alloys. We have to mention a recent measurement[32] of Al-Cu alloys which gives 2.79 Å for the first-shell distance, while our measurement yields 2.725 Å. We think this discrepancy arises partly from the thermal treatment of the samples which in Ref. 32 was not achieved

through a reversion treatment, so that the samples may no longer be a solid solution, as it has been discussed in Ref. 5.

Our new measurement of Al-Mg alloys does support our previous findings, though the ratio of the EXAFS measurement to the value calculated within the continuous elastic theory is smaller for Al-Mg alloys than that for Al-Cu and Al-Zn alloys. We thus can conclude from these direct measurements that the elastic theory of continuous medium cannot be used to calculate the strains around a point defect in a solid solution.

Indeed, this point is probably not restricted to a specific type of point defect, but should also be taken into consideration for interstitials, or even for more extended defects such as GP zones. Besides its theoretical interest, it may be of practical importance in the determination of the structure of defects. Such measurements result usually from the analysis of diffuse x-ray scattering experiments for which one has to substract the strain contribution from the scattering pattern in order to reach the short-range order parameters.[33] Using the elastic theory to calculate such strain effects may give unreliable results, at least when strains are large in the neighborhood of the defect. Just to mention the aluminium dilute alloys, this may be a serious problem in the modeling of GP zones in Al-Cu alloys from x-ray diffuse scattering data, while it should be practically without importance in the case of Al-Zn alloys where strains are weak.

C. Comparison with the lattice static method

This theory tries to take into account the discrete nature of the lattice and to calculate the displacements of the host atoms within the matrix in the neighborhood of a defect. Based upon the Born—von Kármán model of the lattice, it calculates the static response of the lattice to a probe, which is in this case the stresses due to the point defect, using the zero frequency limit of the phonon Green's function. In most calculations it is assumed that the defect interacts directly with only its nearest neighbors or sometimes next nearest neighbors. Even within this restriction, these calculations are not easy to perform since forces are estimated from the derivatives of pairwise potentials. For this estimation Tomlinson *et al.*[8] followed the method developed by Shaw. This method deals with the screening problem and the Friedel oscillations. It is difficult to handle since the phase of the oscillations, and thus the stresses, is very dependent on the model used for the screening. They have calculated the displacements of the four first shells of host atoms about Mg, which they found to be 0.020, 0.0056, 0.0075, and 0.0080 Å, respectively. The displacement of the host atoms in the first shell is very weak compared to the EXAFS measurement, which cannot be interpreted by this calculation. The calculated displacements seem to be very small, indeed too small to produce the rather important change of the lattice parameter which is observed for this solid solution. Thus even if, conceptually, the lattice static method is more satisfactory than the rough theory of continuous elasticity, one has to point out that it does not fit the experimental result, probably because of an incorrect treatment of the pairwise potentials. On the other hand, direct measurements by EXAFS may give accurate values of the core effect, which could be used to fit the potentials be-

TABLE I. Comparison between the EXAFS measurement of the elastic core effect and the value calculated using the elastic continuous theory (CT) for Al-Cu, Al-Zn, and Al-Mg alloys (notations in text).

	$\frac{da}{ac}$ [a]	db'^{∞} (Å)	db(CT) (Å)	db(EXAFS)	$\frac{db(\text{EXAFS})}{db(\text{CT})}$
Al—2 at. % Cu	−0.12	−0.041	−0.043	−0.125±0.01[b]	2.9±0.3
Al—0.83 at. % Zn	−0.02	−0.007	−0.007	−0.02 ±0.01[c]	2.9±1.5
Al—3 at. % Mg			0.038	0.075±0.015	
Al-Mg	+ 0.109	+ 0.035			2.0±0.4
Al—7.3 at. % Mg			0.042	0.085±0.015	

[a]X-ray scattering data (Ref. 31).
[b]Reference 4.
[c]Reference 5.

tween the impurity and the first-shell neighbor atoms.

VI. CONCLUSIONS

In the soft-x-ray range, EXAFS spectra are often restricted to a few hundred electron volts, which makes an accurate analysis of the data difficult. In this work, we only had a signal just over 220 eV, so that special care was needed to extract quasiexperimental phase shifts from both Al and Mg spectra. Thus it has been possible to measure with good accuracy (better than ± 0.02 Å) the Mg—Al distance leading to the "elastic core effect" caused by the Mg atom point defects distorting the host matrix. Provided a comparative method is used to determine accurate phase shifts, the EXAFS technique proves to be a powerful technique for investigating the structure of the defects even when they are built by light elements. The EXAFS measurement yields a large core effect of about 8×10^{-2} Å, which is twice as large as the value that one can derive from the macroscopic effect of change of the lattice parameter using the continuous elastic theory, which is still much larger than the result of a sophisticated calculation using the lattice static method.

Furthermore, these measurements support the previous idea that the continuous elastic theory is not able to supply from macroscopic effects an insight into the displacements of the close host neighbors of a solute atom. Such conclusions should be taken into account for physical measurements when dealing with the lattice distortions.

ACKNOWLEDGMENTS

We would like to thank Professor J. Friedel for enlightening discussions about elasticity in solid solutions. We are also grateful to Mrs. Bizouard for having performed the chemical analysis of the samples and to the staffs of LURE and of the Laboratoire de l'Accélérateur Linéaire for the operation of the ACO storage ring.

---

*Laboratoire propre du CNRS, associé à l'Université de Paris Sud, Orsay.

†Laboratoire de l'Université de Paris Sud, associé au CNRS.

[1]F. W. Lytle, G. H. Via, and J. H. Sinfelt, J. Chem. Phys. 67, 3831 (1977).

[2]E. A. Stern, D. E. Sayers, J. G. Dash, H. Shechter, and B. Bunker, Phys. Rev. Lett. 38, 767 (1977).

[3]S. H. Hunter, A. Bienenstock, and T. M. Hayes, in *Proceedings of the Seventh International Conference on Liquid and Amorphous Semiconductors, Edinburgh, 1977,* edited by W. E. Spear (University of Edinburgh, Edinburgh, 1977), p. 78.

[4]A. Fontaine, P. Lagarde, A. Naudon, D. Raoux, and D. Spanjaard, Philos. Mag. 40, 17 (1979).

[5]J. Mimault, A. Fontaine, P. Lagarde, D. Raoux, A. Sadoc, and D. Spanjaard, J. Phys. F 11, 1311 (1981).

[6]H. Kanzaki, J. Phys. Chem. Solids 2, 24 (1957).

[7]V. K. Tewary, Adv. Phys. 22, 757 (1973).

[8]P. G. Tomlinson, J. P. Carbotte, and G. R. Piercy, J. Phys. F 7, 1305 (1977).

[9]A. Fontaine, P. Lagarde, D. Raoux, and J. M. Esteva, J. Phys. F. 9, 2143 (1979).

[10]A. Dauger, Thèse d'Etat, Université de Poitiers, 1973 (unpublished).

[11]M. Lemonier, O. Collet, C. Depautex, J. M. Esteva, and D. Raoux, Nucl. Instrum. Meth. 152, 109 (1978).

[12]D. E. Sayers, E. A. Stern, and F. W. Lytle, Adv. X-ray Anal. 13, 248 (1970).

[13]E. A. Stern, Phys. Rev. B 10, 3027 (1974).

[14]C. A. Ashley and S. Doniach, Phys. Rev. B 11, 1279 (1975).

[15]B. K. Teo and P. A. Lee, J. Am. Chem. Soc. 101, 2815 (1979).

[16]P. A. Lee and J. B. Pendry, Phys. Rev. B 11, 2795 (1975).

[17]R. F. Pettifer and P. W. McMillan, Philos. Mag. 35, 879 (1977).

[18]C. Noguera, D. Spanjaard, and J. Friedel, J. Phys. F. 9, 1189 (1979).

[19]P. A. Lee and G. Beni, Phys. Rev. B 15, 2862 (1977).

[20]P. H. Citrin, P. Eisenberger, and B. M. Kincaid, Phys. Rev. Lett. 36, 1346 (1976).

[21]D. Raoux, J. Petiau, P. Bondot, G. Calas, A. Fontaine, P. Lagarde, P. Levitz, G. Loupias, and A. Sadoc, Rev. Phys. Appl. 15, 1079 (1980).

[22]P. Eisenberger and G. S. Brown, Solid State Commun. 29, 481 (1979).

[23]G. Martens, P. Rabe, N. Schwentner, and A. Werner, Phys. Rev. B 17, 1481 (1978).

[24]A. Dauger, J. P. Guillot, and J. Caisso, Acta Metall. 22, 733 (1974).

[25]M. Bernole, R. Graf, and P. Guyot, Philos. Mag. 28, 771 (1973).

[26]J. Friedel, Philos. Mag. 46, 514 (1955).

[27]J. D. Eshelby, in *Solid State Physics,* edited by F. Seitz, H. Ehrenreich, and D. Turnbull (Academic, New York, 1956), Vol. 3, p. 79.

[28]A. Blandin and J. L. Deplante, J. Phys. Chem. Solids 26, 3819 (1963).

[29]J. L. Deplante, Thèse de 3ème cycle, Université de Paris, 1963 (unpublished).

[30]K. A. Gschneider, in *Solid State Physics,* edited by F. Seitz, H. Ehrenreich, and D. Turnbull (Academic, New York, 1964), Vol. 16, p. 275.

[31]W. B. Pearson, *Handbook of Lattice Spacings and Structure of Metals* (Pergamon, New York, 1958), Vol. 4.

[32]B. Lengeler and P. Eisenberger, Phys. Rev. B 21, 4507 (1980).

[33]A. Guinier, *Theorie et Technique de la Radiocristallographie* (Dunod, Paris, 1956).

[34]M. Roth and J. M. Raynal, J. Appl. Cryst. 7, 219 (1974).